12-9-2006

Innovative Scintillating Optical Fibers For Detecting/Monitoring Gamma Radiation

Ashwini Jayaprakash

INNOVATIVE SCINTILLATING OPTICAL FIBERS FOR DETECTING/MONITORING GAMMA RADIATION

By

Ashwini Jayaprakash

A Thesis
Submitted to the Faculty of
Mississippi State University
In Partial Fulfillment of the Requirements
For the Degree of Master of Science
in Physics
in the Department of Physics and Astronomy

Mississippi State, Mississippi

December 2006

INNOVATIVE SCINTILLATING OPTICAL FIBERS FOR DETECTING/MONITORING GAMMA RADIATION

By

Ashwini Jayaprakash

Approved:

_____	_____
Shiquan Tao Associate Research Professor, Institute for Clean Energy Technology (Director of Dissertation)	David L Monts Professor of Physics and Astronomy and Graduate Coordinator of Department of Physics and Astronomy (Committee Member)
_____	_____
Wenchao Ma Professor of Physics Department of Physics and Astronomy (Committee Member)	Philip B. Oldham Dean of College of Arts and Sciences

Name: Ashwini Jayaprakash

Date of Degree: December 9, 2006

Institution: Mississippi State University

Major Field: Physics

Major Professor: Dr. Shiquan Tao

Title of Study: INNOVATIVE SCINTILLATING OPTICAL FIBERS FOR DETECTING/MONITORING GAMMA RADIATION

Pages in Study: 58

Candidate for Degree of Master of Science

A scintillating optical fiber sensor of this work consists of a scintillating optical fiber, connected to a photomultiplier tube (PMT) via a conventional silica optical fiber. When a gamma ray impinges on the scintillating optical fiber, photons are generated inside the fiber. The photons are trapped inside the fiber and guided through the PMT. The PMT output signal is acquired by a computer. Two types of scintillating optical fibers sensors were developed for gamma ray detection. The first one is a silica optical fiber doped with an inorganic scintillating agent. The second one is a liquid core waveguide optical fiber filled with a solution of a nanostructured core shell CdSe/ZnS quantum dot.

Test results indicate that the scintillating optical fibers developed in this work are sensitive for detecting gamma radiation. These scintillating fibers offer more flexibility for applications in nuclear energy industry as well as in nuclear medical research.

ACKNOWLEDGEMENTS

I would like to take this opportunity to express my sincere thanks to my research advisor, Dr. Shiquan Tao for all his guidance, direction and support during the evolvement of this thesis. I truly want to thank him for hiring me as a research assistant and for all the training he provided.

I am totally indebted to Dr. David L Monts, graduate coordinator and my committee member for all his help and resourceful suggestions. Sincere appreciation is extended to Dr. Wenchao Ma, for serving as my committee member and for all the instructions.

Finally, I would like to acknowledge my parents for always standing by me.

TABLE OF CONTENTS

Page

ACKNOWLEDGEMENTS ii

LIST OF TABLES v

LIST OF FIGURES vi

CHAPTER

I. INTRODUCTION 1

Sources of Gamma Rays 1
Health Effects from Radiation Exposures 2
Gamma Radiation Detectors 3
Gas-Filled Detectors 3
Semiconductor Detectors 6
Scintillating Detectors 7

II. TYPES OF SCINTILLATORS 8

Organic Scintillators 8
Inorganic Scintillators 10
Basic Principles of Scintillating Mechanism 11
Scintillation Mechanism in Organic Scintillators 18
Scintillation Mechanism in Inorganic Scintillators 21

III. OBJECTIVE 25

Approach 25
Sol-Gel Technique 26
Sol-Gel Process 26
Optical Properties of Sol-Gel Silica 28
Sol-Gel Derived Materials 29
Sol-Gel Derived Hybrid Materials 30
Applications 31

IV. SEMICONDUCTOR QUANTUM DOT 33

CHAPTER Page

Advantages of Using Quantum Dot 35
Applications 36

V. PREPARATION OF SCINTILLATING FIBERS 37

Preparation of Liquid Core Waveguide Fiber 37
Liquid Core Waveguide Detector Probe 37
Preparation of CsI and NaI Doped Silica Scintillating Fibers 38
CsI/NaI Doped Silica Fiber Probe Detector 39
Connecting a Scintillating Optical Fiber Sensor Probe to a PMT 39

VI. EXPERIMENTAL SET-UP 41

VII. RESULTS AND DISCUSSION 43

Calibration 51

VIII. POTENTIAL APPLICATIONS OF THE SCINTILLATING FIBER DETECTOR 55

REFERENCES 57

LIST OF TABLES

TABLE Page

7.1 Test Results of Scintillating Fibers as Recorded from HC135-11 PMT Module 44

7.2 Detection Limits Obtained for the Tested Scintillating Fibers of this Work 51

LIST OF FIGURES

FIGURE		Page
1.1	Basic circuit for gas-filled detector	4
2.1	A single peak which represents the total electron energy corresponding to the gamma radiation	12
2.2	Compton scattering	13
2.3	Pair production	14
2.4	Schematic of photon transit from a scintillating material to PMT	18
2.5	The π-electron structure of organic scintillators showing the energy levels	20
2.6	Energy states showing full valence band and empty conduction band	22
2.7	Energy band structure of an inorganic crystal scintillator with activator	24
3.1	The light transmission of porous silica. The transmission in the graph is the fraction of light intensity transmitted through porous silica	29
4.1	Absorption and photoluminescence spectra of the CdSe and Cdse/ZnS core-shell nanocrystals	34
4.2	Overview and high resolution transmission electron microscope of a) CdSe and b) CdSe/ZnS core-shell nanocrystals..	35
5.1	Liquid core scintillating fiber detector probe	38
5.2	CsI/NaI doped silica scintillating fiber detector probe	39
5.3	A circuit diagram of PMT module connected to a computer	40

FIGURE Page

6.1 Schematic of the experimental set-up 42

7.1 Radiation counts (Roentgen/Hr) of Fluoranthene liquid core scintillating fiber 46

7.2 Radiation counts (Roentgen/Hr) of Anthracene liquid core scintillating fiber 46

7.3 Radiation counts (Roentgen/Hr) of Quantum Dot liquid core scintillating fiber 47

7.4 Radiation counts (Roentgen/Hr) of Commercial scintillating fiber 47

7.5 Radiation counts (Roentgen/Hr) of NaI doped silica scintillating fiber 49

7.6 Radiation counts (Roentgen/Hr) of CsI doped silica scintillating fiber 49

7.7 Radiation counts (Roentgen/Hr) of CsI(NaI) doped silica scintillating fiber 50

7.8 Radiation counts (Roentgen/Hr) of CsI doped silica scintillating fiber with different concentrations 50

7.9 A calibration curve of Commercial scintillating fiber for detecting gamma radiation quantitatively 52

7.10 A calibration curve of NaI doped silica scintillating fiber for detecting gamma radiation quantitatively 52

7.11 A calibration curve of CsI(Na) doped silica scintillating fiber for detecting gamma radiation quantitatively 53

7.12 A calibration curve of CsI doped silica scintillating fiber for detecting gamma radiation quantitatively 53

7.13 A calibration curve of Quantum Dot solution filled scintillating fiber for detecting gamma radiation quantitatively 54

CHAPTER I

INTRODUCTION

Gamma rays have the smallest wavelengths and the most energy of any other wave in the electromagnetic spectrum. They are often defined to begin at an energy of 10 keV upto several hundred MeV. They are emitted from the excited nuclei in their transition to lower lying nuclear levels. They are more penetrating than alpha and beta rays but less ionizing. They are same as X-rays, while X-ray is a term for high-energy electromagnetic radiation produced by energy transitions due to accelerating electrons, gamma rays originate in the nucleus.

Sources of Gamma Rays

Gamma rays are often produced alongside other forms of radiation such as alpha or beta. When a nucleus emits an α or β particle, the daughter nucleus is sometimes left in an excited state. It can then jump down to a lower level by emitting a gamma ray in much the same way that an atomic electron can jump to a lower level by emitting visible light or ultraviolet radiation.

Most people's primary source of gamma exposure is naturally occurring radionuclides, particularly potassium-40, which is found in soil and water, as well as eats and high-potassium foods such as bananas. Radium is also a source of gamma exposure.

However, the increasing use of nuclear medicine (e.g., bone, thyroid, and lung scans) contributes an increasing proportion of the total exposure dose for many people.

There are many sources of gamma radiation the primary one being naturally occurring radionuclides like uranium, thorium, radium and unstable man-made isotopes like ^{60}Co, ^{22}Na, ^{133}Ba, ^{99}TC, etc. The gamma source used in this experimental work is ^{137}Cs. Cesium-137 is a radioactive element with a half-life of thirty years. It decays to ^{137}Ba, which has a very short lifetime. The radioactive decay of ^{137}Cs has two components. First the neutron inside the ^{137}Cs nucleus undergoes beta decay converting the neutron into proton and a beta particle (electron) and a neutrino. The ^{137}Ba nucleus is left in the excited state at an energy of 662KeV above the ground state. When this level decays, 662KeV gamma ray is emitted. The half-life of ^{137}Ba is determined. Finally the ^{137}Ba becomes stable with a mass of 137, consisting of 56 protons and 81 neutrons.

Health Effects from Radiation Exposures

a) Acute Effects

It is a single accidental exposure to a high dose of radiation during a short period of time. Acute radiation overexposure affects all the organs and systems of the body. However not all organs systems will be equally exposed to radiation. These effects may cause nausea and vomiting, malaise and fatigue, increased temperature and blood changes and non-cancerous skin damage.

b) Chronic Effects

These are long term, low level overexposure of radiation exposure. These effects can be caused due to exposure to external radiation fields, or can result from inhalation or ingestion of a radioisotope. Chronic effects can cause radiation induced cancer in the skin, the hemopoietic system, the bone, and the thyroid gland. In all these cases the tumor induction time in man is relatively long, in the order of 5 to 20 years for after exposure. Chronic effects due to long term radiation exposures can also cause genetic disorders by affecting the gene carrying chromosomes [1].

Gamma Radiation Detectors

Radiation detectors are devices that measure the ionization energy and produce an observable output. The basic requirements of any radiation measuring instrument is that the magnitude of the instrument's response is proportional to the radiation effect or radiation property under measurement [2].

Gas-Filled Detectors

The general circuit of a gas-filled detector is shown in Figure 1.1. This system consists of a variable voltage source V, a high valued resistor R, and a gas filled counting chamber, which has two coaxial electrodes that are very well insulated from each other.

All the capacitance associated with the circuit is given by capacitor C. Because of the production of ions within the detector when it is exposed to radiation, the gas within the detector becomes electrically conducting. If the constant RC of the detector circuit is

much greater than the time required for the collection of all ions resulting from the passage of a single particle through the detector then a voltage pulse of magnitude

$$V=\frac{Q}{C} \tag{1.1}$$

where, Q is the total charge collected and C is the capacitance of the circuit, appears across the output of the detector circuit [1].

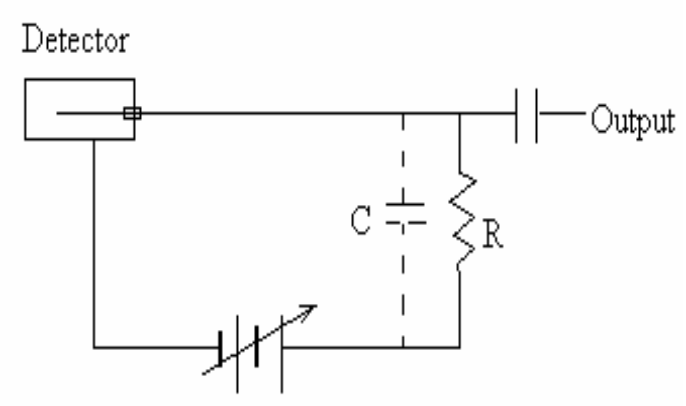

Figure 1.1: Basic circuit for gas-filled detector

There are three main types of gas filled detectors:

1) Geiger Muller Counter

In the Geiger region all detected pulses, regardless of their initial energy, have the same energy output since the overall amplified energy caused by a given pulse, regardless of it initial magnitude, is limited only by circuit and tube constants. Such a tube cannot be used as a radiation or pulse discriminant, although counting in this range permits detection of the least amount of energy released pulse.

Since each ionizing event eventually results in ionization of a significant fraction of the gaseous molecules in the detector, the ions thus produced must be swept from the detector before a succeeding ionizing event can produce a pulse. This time delay, sometimes called dead time, determines the frequency of the ionizing events that can be detected and thus an average resolving time of the unit.

Measurements with such detectors reflect only the number of incident particles regardless of the total ionization energy [2].

2) Ionization Chamber

The ions produced by ionization in the chamber itself are collected on walls, and the resulting charge is measured by an auxiliary circuit [2]. The number of electrons collected by the anode will be equal to the number produced by the primary ionizing particle. The pulse size will therefore be independent of the voltage, and will depend only on the number of ions produced by the primary ionizing particle during its passage thought he detector. The ionization chamber region may be defined as the range of operating voltages in which there is no multiplication of ions due to secondary ionization; that is, the gas amplification factor is one. The fact that the pulse size from the counter operating in the ionization chamber region depends on the number of ions produced in the chamber makes it possible to use this instrument to distinguish between radiations of different specific ionization, such as alphas and betas or gammas [1].

These detectors have slow response times. They are generally insensitive to low levels of radiation and sensitive to the effects of temperature, pressure, and humidity changes.

3) Proportional Counters

As the voltage across the counter is increased beyond the ionization chamber region, appoint is reached where secondary electrons are produced by collision. The gas multiplication factor is greater than one. This multiplication of ions in the gas, which is called an avalanche, is restricted the vicinity of the primary ionization. Increasing the voltage causes the avalanche to increase in size by spreading out along the anode. Since the size of the output pulse is determined by the number of electrons collected by the anode, the size of the output pulse from a given detector is proportional to the high voltage across the detector. For the purpose of distinguishing between radiations the counter depends on the pulse size of ionization and therefore maybe operated as a proportional counter [1].

Semiconductor Detectors

Semiconductor detectors generally use germanium or silicon as the semiconducting material. These detectors have a *p* or *n*-type diode. Intrinsic charge carriers create the depletion region when a reverse bias is applied across the diode. When photons interact within the depletion region, charge carriers (holes and electrons) are free to move towards their respective electrode by the electric field. A semiconductor with an excess number of electrons is called *n*-type semiconductor while with an excess of holes is called *p*-type semiconductor. The resultant charge is amplified and converted to a voltage pulse with an amplitude proportional to the original ionization energy. It offers good energy resolution but the main problem of germanium detectors is the necessity for

cryogenic cooling and stabilizing the detector at a temperature near the liquid nitrogen (around 77°K or -200°C) to reduce thermal noise and radiation damage [3].

Scintillating Detectors

A scintillation detector is a device that emits photons when ionizing radiation interacts with the detector. The photons are converted into an electrical signal and recorded on a photodetector. The photodetector commonly used is a photomultipler tube (PMT), which consists of a photocathode and several dynodes, which multiply the electrons to yield a current pulse. This current pulse is amplified and can be digitized to give counts that can be measured. The amount of photons is proportional to the amount of energy deposited. A wide variety of crystal scintillators are available, examples include thallium activated NaI and CsI crystals, bismuth germanate (BGO) calcium fluoride activated by Europium **(**CaF:Eu**),** Gadolinium silicate doped with cerium (GSO)**,** Cadmium tungstate ($CdWO_4$), etc. The crystals are in the form of plates, rods and image screens and coupled to optical fibers.

Most scintillating detectors make use of crystal scintillators, which have the highest efficiency. But in these crystals only a small amount of emitted light reaches the photodetector directly. Most of the light encounters one or more reflections on lateral surfaces before being detected, especially the long crystals. In the case of long bare crystal, the light should undergo total internal reflection to have a reasonable chance to reach the photodetector [4].

CHAPTER II

TYPES OF SCINTILLATORS

Many materials scintillate at some level.Scintillators can be broadly classified as : 1) Organic and 2) Inorganic scintillators

Organic Scintillators

Organic Crystalline Scintillators

These are organic molecules, which have an aromatic ring. They are characterized by a fast response, in the order of one nanosecond. When pure, they form crystals, which are difficult to shape.

Anthracene is one of the best known organic scintillator with good energy resolution and maximum quantum efficiency of 90%. Napthalene is an organic scintillator whose relative response to different ionizing particles is similar to that of Anthracene [3]. Stilbene is a crystal scintillator with high scintillation efficiency and short scintillation decay time. In organic scintillators light emission occurs as a result of fluorescence where the molecule gets excited by energy absorption from ionizing radiation particles. The scintillation response of organic phosphors to heavy particles is less compared to electrons of equal energy. Here the fluorescence excitation by ionizing

particles is less compared to photo-excitation since much of the energy of incident particle is dissipated as heat [3, 5].

Organic Liquid Scintillators

The organic crystal scintillator can be dissolved in an organic solvent, for example in xylene, toulene and mineral oil, maintaining properties similar to the organic crystal, depending on purity and concentration they form liquid scintillators. The ionizing particle produces primary photons by the ion recombination and high excitation of the solvent molecules. The decay time of this process is hence shorter than in solids due to increased molecular collisions. Some of these primary photons wills be absorbed by the solute molecules, which trap energy and subsequently re-emit their characteristic fluorescence. Also the primary photons absorbed by the solvent molecules will cause them to fluoresce provided the internal quenching is not too great, and this solvent emission will be preferentially absorbed by the solute molecules giving fluorescence. Thus energy may be transferred by photons over a wide spectral region unto the longest wavelengths of the solvent fluorescence. The processes that occur after the primary emission are those of photofluorescence [5].

Plastic Scintillators

These are organic scintillators dissolved in organic monomer, which is polymerized to form plastic scintillators. When organic scintillator is dissolved in a transparent solvent like polystyrene and then polymerized it forms a solid solution of plastic scintillators. Here the fluorescence is due to the initial excitation of the solvent (polystyrene) molecules, emitting photons. These photons are completely reabsorbed by

the solute molecules and that the emission is entirely from the solute organic scintillator which makes them entirely transparent [3, 5]. They suffer from ageing, due to the formation of minute surface cracks (crazing) and radiation damage, which darkens the plastic at a level of about 10^3 Gy.

Inorganic Scintillators

These scintillators are used where high density and good energy resolution are required. They are characterized by a high stopping power due to their high atomic no. Z, which makes them most appropriate to detect high energy radiation. But they have longer decay times, in the order of hundreds of nanoseconds. There are three main classes of inorganic scintillators:

i)Activated scintillators, such as NaI:Tl which has light output of 2.3 times that of anthracence, CsI: Na, CaF_2:Eu and Lu_2SiO_5:Ce, where the ionizing energy diffuses through the host crystal and produces an excited state at or near an activator atom that is present in low concentrations(typically~0.1%)

ii)Self activated scitillators, such as CsI,NaI,$Bi_4Ge_3O_{12}$, BaF_2 and $PbWO_4$, where the activator atoms are a major constituent of the crystal and /or excitonic process are involved.

iii)Core valence luminescence scitillators, such as BaF_2,CsF and $RbCaF_3$, where the ionizing radiation produces an electron vacancy in an upper core level of one atom and the vacancy use promptly (≈ 1ns) filled with an electron from the valence band of another atom to produce light[19].

Basic Principles of Scintillation Process

The operation of a scintillation counter can be divided into five stages:

1) The absorption of the incident radiation and creation of primary electrons and holes

2) The luminescent conversion of dissipated energy and emission of photons

3) The photon transit to the cathode of the photomultiplier tube

4) Absorption of photons at the cathode and conversion into photoelectrons

5) The electron multiplication process

1) Absorption of incident radiation and creation of primary electrons and holes

When a charged particle hits a scintillating particle it dissipates its energy while passing through it. This energy transfer process takes place within 10^{-9} sec or probably less. The total energy from the high energy radiation maybe completely absorbed by the scintillating material or only a small portion may result in light emission. The gamma ray can transfer its energy to the scintillating material by the following process:

a) Photoelectric absorption

This happens at low γ-ray energies when the γ-ray photon interacts with a tightly bound atomic electron. A photoelectron is produced from one of the electron shells (usually K-shell) of the absorber atom with energy a kinetic energy E_e

$$E_e = h\nu \tag{2.1}$$

where $h\nu$ is the absorbed photon energy and E_b is the binding energy of the photoelectron in its original shell. When the photoelectron is ejected a vacancy is created in the atomic orbital, which is filled with an electron from a higher atomic orbit. This results in the

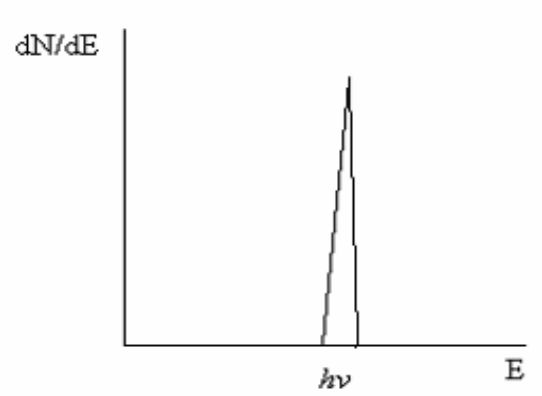

Figure 2.1: A single peak which represents the total electron energy corresponding to the gamma radiation

emission of an X-ray, which might be absorbed in the material. If nothing escapes from the detector then the sum of the kinetic energies of the electrons equals the electrons that are created must equal the original energy of the incident gamma ray photon. The differential distribution of electron kinetic energy for a series of photoelectric absorption events can be represented by a simple delta function.

b) Compton Scattering

This process occurs at intermediate energies (0.5 to 3.5 MeV), when an incident γ-ray scatters from a loosely bound electron in the absorbing material. This results in a recoil electron and scattered gamma ray photon. This photon is of longer wavelength and has less energy than the incident photon. The division of scattered energy and the wavelength shift is dependent on the scattering angle.

The energy of the scattered gamma ray $h\nu'$ in terms of scattered angle is given by:

$$h\nu' = \frac{h\upsilon}{1+\left(\frac{h\nu}{m_0 c^2}\right)(1-\cos\theta)} \tag{2.2}$$

where m_0c^2 is the rest mass energy of the electron. The kinetic energy of the recoil electron is given by:

$$E=hv-hv' = hv\left\{\frac{\frac{hv}{m_0c^2}(1-\cos\theta)}{1+\left(\frac{hv}{m_0c^2}\right)(1-\cos\theta)}\right\} \quad (2.3)$$

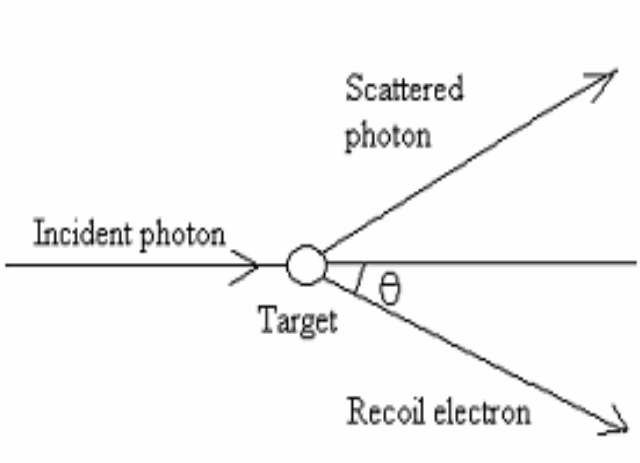

Figure 2.2: Compton scattering

The scattering angle has two possibilities:

1. when $\theta \approx 0$, $hv \approx hv'$ and $E_{e-} \approx 0$, then the recoil electron has very little energy and the scattered photon has nearly the same energy as the incident gamma ray.

2. when $\theta=\Pi$, the incident gamma ray is backscattered towards its direction of origin and electron recoils along the direction of incidence. This case represents the maximum energy that can be transferred to an electron.

Apart from the two cases mentioned all scattering angle will occur in a detector referring to a continuum of energies that is transferred to an electron ranging from zero upto a maximum [5].

c) Pair production

This process occurs at higher energies where the incident γ-ray photon is used for production of mass of an electron-positron pair (E= $2m_0c^2$=1.02MeV where m_0c^2=0.52MeV is the rest mass of the electron). If the incident γ-ray energy exceeds this value of E, then the excess energy appears in the form of residual energy shared between these electron- positron pair.

$$E_p = E_I - 2m_0c^2 \tag{2.4}$$

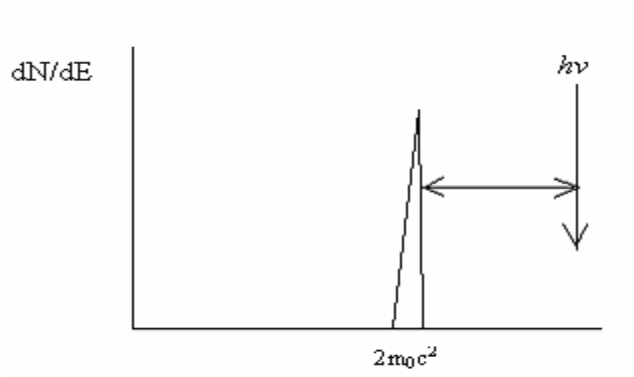

Figure 2.3: Pair production

As the positron slows down, further annihilation takes place resulting in the production of two photons of equal energy (511 keV).

The absorption co-efficients μ_{ph}, μ_c and μ_p corresponding to the above three processes are related as:

$$\mu = \mu_{ph} + \mu_c + \mu_p. \tag{2.5}$$

The magnitudes of these three co- efficients depend on the incident radiation, density of the scintillating material and the atomic number and mass of its constituent elements [5].

2) The luminescent conversion of dissipated energy and emission of photons

An atom with an inner relaxed shell can be relaxed either radiatively by emitting a photon or nonradiatively by generating a secondary electron (Auger effect). Usually the probability of nonradiative decay is much greater that that of radiative decay [18]. The energy might be dissipated in the ionization, excitation and possible dissociation of the molecules of the scintillating material. In a non-luminescent solid or liquid, the whole of this molecular energy is transferred into thermal, vibrational and translational energy and the molecules return to the ground state by radiationless transitions. Whereas in a scintillating material part of the excitation energy is re-emitted as photons of frequency υ_p, energy E_p ($=h\upsilon_p$), wavelength λ_p ($=c/\upsilon_p$) corresponding to direct energy transitions from an excited electronic level to the ground state. The photon emission is not spontaneous. The rate of photon emission decays exponentially with a decay period τ from its maximum intensity I_0.The intensity I after a time t is given by:

$$I=I_0 \exp(-t/\tau) \tag{2.6}$$

The number of electrons emitted in the time interval t is:

$$p_t = p\,[1- \exp(-t/\tau)] \tag{2.7}$$

Thus the relaxation of an atom with a hole occurs as a series of nonradiative and radiative transitions in a time of 10^{-13} to 10^{-15}secs.

3) The photon transit to the cathode of the photomultiplier tube

For maximum light efficiency it is desirable that the scintillating fibers have high optical transparency T_p to it own fluorescence radiation to minimize the number of

scintillation photons absorbed within the scintillating material. For a scintillator of optical absorption coefficient μ and a light path of length x,

$$T_p=e^{-\mu x} \tag{2.8}$$

The light path x usually exceeds the thickness of the scintillator since part of light emitted may undergo successive internal reflections before impinging on the photo-cathode. The absorption coefficient μ should be as small as possible otherwise it would result in overlap of emission and absorption spectra. This would result in loss by absorption of photons emitted in this region. Even for a perfectly transparent scintillator ($T_p=1$) only a fraction G (about 25%) of the photons produced in the scintillator reach the photomultiplier cathode. This fraction G depends on the geometry of the system and the effective solid angle subtended by the scintillator at the photo-cathode. The number of photons incident on the photo-cathode is given by [5],

$$p`=T_pG_p \tag{2.9}$$

4) Absorption of photons at the cathode and conversion into photoelectrons

Firstly the incident light photons are absorbed and their energy ($h\upsilon$) is transferred to the electrons within the photoemissive material. Secondly these electrons migrate to the surface losing its energy through electron-electron collision. Finally the electrons escape from the surface of the photocathode.

There should be sufficient energy for the electrons to overcome the potential barrier existing between the material and vacuum. This potential barrier is normally greater than 3-4 eV for most metals but around 1.5-2 eV for semiconductors. The

sensitivity of the photo-cathodes is given by the quantum efficiency, which is simply equal to:

$$QE=\frac{\text{number of photoelectrons emitted}}{\text{number of incident photons}} \tag{2.10}$$

5) The electron multiplication process

Electrons from the photocathode are accelerated and caused to strike the surface of an electrode called a dynode. These electrons have a kinetic energy of the order of 1eV or less. Therefore the first dynode is held at a positive potential of several hundred volts. The average energy required to excite an electron within the dynode material should be equal to the bandgap, which is of the order 2-3eV causing the release of nearly 3 electrons per volt applied. Because the electrons are moving randomly inside the PMT many will not reach the surface before their de-excitation or they lose energy to overcome the potential barrier at the surface. Hence only a small fraction of excited electrons contribute to the secondary electron yield from the dynode surface. If there are *n* dynodes, each with an electron multiplication factor R, the overall gain of the tube is:

$$\text{Gain}=CR^{n} \tag{2.11}$$

where C is the collection efficiency factor of the photoelectrons by the dynode system and multiplication factor is [5]:

$$R=\frac{\text{number of secondary electrons emitted}}{\text{primary incident electron}} \tag{2.12}$$

The electrons have a definite transit time t_T through the photomultiplier tube. It is the average time difference between the arrival of a photon at the photocathode and the

collection of the subsequent electron burst at the anode. It ranges from 20 to 80 ns for different photomultiplier tubes [3].

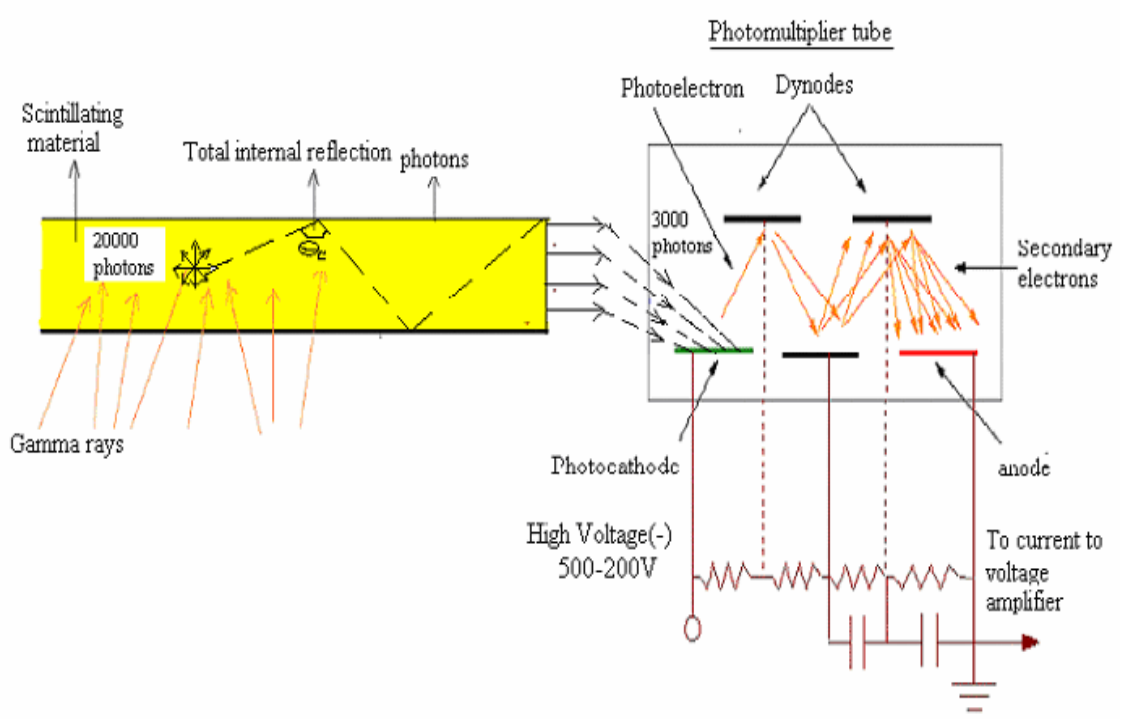

Figure 2.4 Schematic of photon transit from a scintillating material to PMT

Scintillation Mechanism in Organic Scintillators

The manner in which particle energy is dissipated as ionization and excitation in a scintillator appears as visible light is essentially different in organic, as compared to inorganic materials. When the scintillating material absorbs the radiation energy, the high-energy particles or photons collide with the electrons in the material. The electrons become excited and jump to higher energy states. Since the electrons in the excited state have the same spin as they did in the ground state, they are not stable and almost

spontaneously become de-excited to lower energy levels, releasing energy in the form of light. This phenomenon is known as fluorescence, which is an “allowed” transition. When the excited state is meta-stable then light emission continues even after the source of energy is removed. These excited states give rise to electron transitions to lower energy states resulting in phosphorescence. Here the direct transition to the ground state is “forbidden” [5].

Fluorescence

As shown in the Figure 2.5, the organic molecules have symmetric properties related to π – electron structure, where regions 1 and 2 represent absorption, 3 fluorescence, 4 inter-system crossing and 5 phosphorescence. A series of singlet state with spin 0 are shown as $S_0, S_1, S_2 \ldots$ a series of triplet state with spin 1 as $T_1, T_2, T_3 \ldots$

These electronic configurations are further subdivided into levels with smaller spacing such as S_{00}, S_{01}, S_{02} and so on corresponding to vibrational state of the molecules. The lowest vibrational state of the ground electronic state is represented by S_{00}.

Before the excitation of electrons, they are in the lowest vibrational level of the ground electronic state. Absorbing the kinetic energy of the charged particle excites the electrons, allowing them to enter a higher vibrational level in the excited state. The electrons in higher singlet excited states are quickly de-excited to the S_1 electron state through radiationless transfer or quenching. Any higher state such as S_{11}, S_{22} in not in thermal equilibrium with its neighbors and again loses that vibrational energy.

The electrons in the excited state have the same spin as they did in the ground state. The electrons in S_{10} state jump back to the ground state, re-entering it first at a

higher vibrational level before losing the excess vibrational energy in the form of scintillating light.

The wavelength of light absorbed for excitation will be shorter than the wavelength emitted during de-excitation. (Stokes' law). The fluorescence decays exponentially with a decay time τ and the intensity I after a time t is given by:

$$I=I_0 e^{-t/\tau} \tag{2.13}$$

This fluorescent state can exist for a few nanoseconds [3].

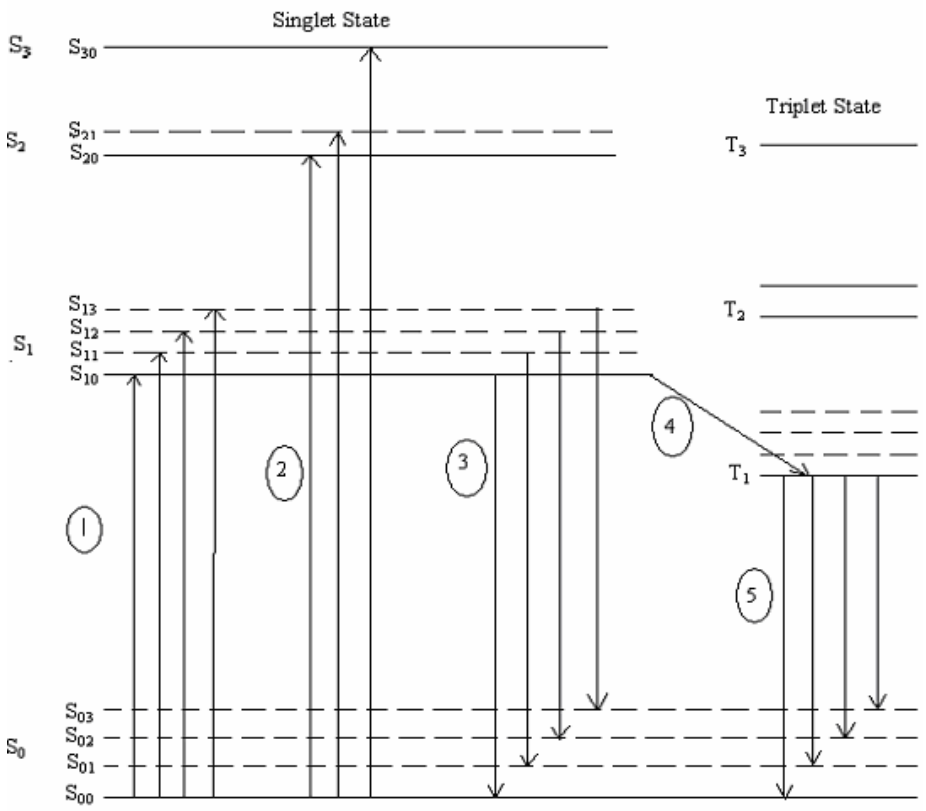

Figure 2.5: The π-electron structure of organic scintillators showing the energy levels

Phosphorescence

In this process light emitted by an atom or molecule persists after the exciting source is removed. While excited, the electrons experience a change in spin called intersystem crossing where some excited singlet states may be converted to triplet states. This change in spin places the electrons in a metastable position forbidding them to move back into the ground state. Thermal energy from within the crystal structure releases the electron from the troughs, which causes them to be raised to a higher, less stable energy level where they can eventually fall back to lower energy levels. During this de-excitation from T_1 to S_0 there is delayed light emission known as phosphorescence. Phosphorescent states can exist from 10^{-4} seconds to several hours and wavelength maybe longer than that of fluorescence spectrum.

We thus see that scintillation in organic materials is inherently a molecular property and is exhibited in liquid and solid solutions, and in the solid, liquid, vapor, plastic and glassy states [3, 5].

Scintillation Mechanism in Inorganic Scintillators

The mechanism of scintillation of an inorganic substance is the result of impurities or defects in the crystalline lattice, rather than a property of individual molecules. The energy state of an inorganic scintillator material consists of a valence band, conduction band and forbidden band. When no energy is absorbed the lower valence band is completely filled with electrons bound at lattice sites. At room temperatures, there is some smearing of the energy distribution of the electrons, such that

a small, but not insignificant number have enough energy to cross the energy band gap into the conduction band. The intermediate forbidden band consists of no electrons. These bands extend throughout the crystal and hence the scintillation depends on the crystal lattice of the material.

When the scintillator absorbs radiation energy the electrons are excited and elevate to the conduction band from the valence band, creating holes in the valence band. The electrons falling back to valence band emit high-energy photon, which would lie beyond the visible region for a pure crystal. This band gap needs to be reduced in order to lower the energy of the emitted photon to the visible range. When small amount of impurity called activators are added to the inorganic scintillator, it creates energy states within the

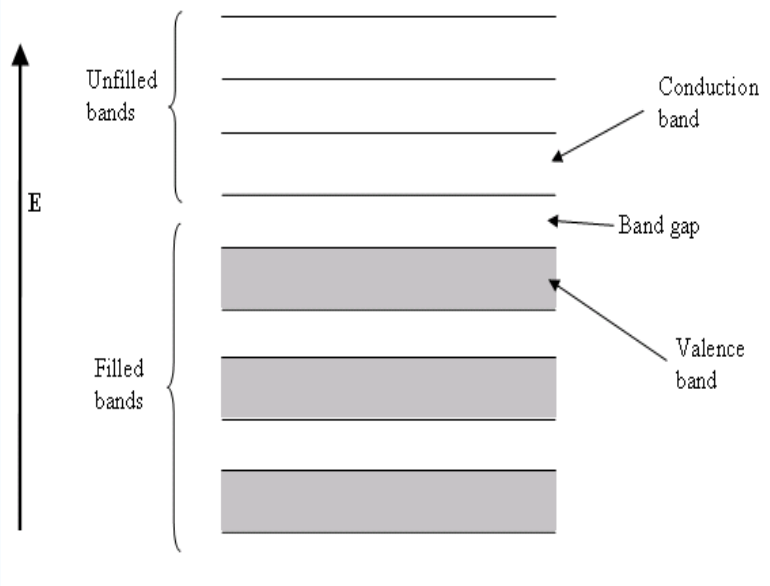

Figure 2.6: Energy states showing full valence band and empty conduction band

forbidden band through which the electron can de-excite back to the valence band, thus increasing the probability of visible photon emission during de-excitation.

When ionizing radiation strikes the scintillator material , it excites an electron out of its energy level consequently leave a hole and creating electron-hole pairs. These holes which act like positive charge drift towards an activator site and ionize it. A positive electric charge is produced when an electron bound to an atom or molecule absorbs enough energy from an external source to escape from the electric potential barrier that originally confined it. This happens because the ionization energy of the activator is less than the positive hole. When a free electron migrate towards a ionized activator it form a neutral state having its own energy states. Now, the scintillation occurs through the de-excitation of the activators to the ground state by the emission of photons. This transition will occur in the visile range with the half lives being in the order of 10^{-7}s.

There is possibility of quenching mechansim taking place when the electron gets trapped in the activator site and the de-excitation to the ground state produces radiationless transitions or no visible photons.

A third possibility exists when an electron reaches a metastable state and may jump back to the conduction band acquiring thermal energy from the lattice vibrations and then de-excite to the ground state giving rise to a slow component of light called phosphorescence [3, 5].

Properties required for a good scintillator

- High scintillation efficiency
- Fast scintillation, decay time of induced luminescence should be short

- Linear energy conversion
- The scintillating material should be transparent for maximum light collection
- The refractive index should be similar to that of glass (~1.5)
- High density and high atomic number for good photoelectric absorption

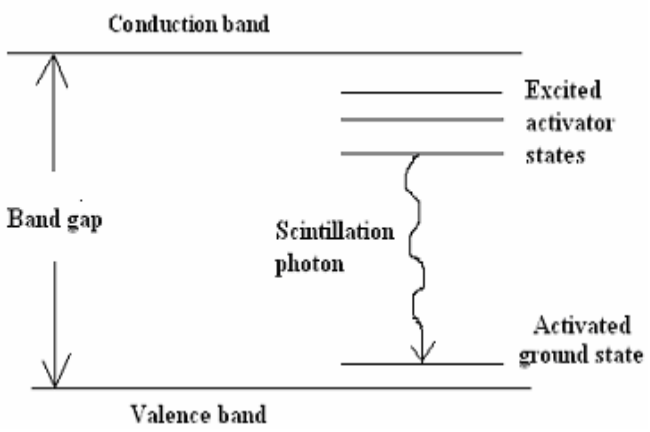

Figure 2.7: Energy band structure of an inorganic crystal scintillator with activator

CHAPTER III

OBJECTIVE

Among the scintillating materials, inorganic scintillators have the highest efficiency and energy resolution for gamma ray detection. However, the inorganic scintillators are presently in the form of crystals or coating. The crystals are expensive; need extensive care in handling and operation. In addition, it is difficult to make large crystal detectors. The plastic scintillators are robust, can be made into desired shape and can be made in large size. However, these scintillators have low efficiency and low energy resolution. Therefore, new technologies for making inorganic materials, which have flexible properties similar to that of plastic scintillators, are highly desired in order to design new scintillating detectors for application in DoD' s field tasks.

Approach

Two approaches have been incorporated in making scintillating optical fibers. The first scintillating optical fiber is a sol-gel derived silica optical fiber doped with an inorganic scintillating agent like CsI and NaI. The second scintillating optical fiber is a liquid core waveguide optical fiber filled with a solution of a nanostructured core shell CdSe/ZnS quantum dot. Scintillating optical fiber sensors have been constructed by using these scintillating optical fibers as transducers.

Sol-Gel Technique

The sol-gel process is a technique used for the production of ceramic materials. Sol can be created by either organic or inorganic precursors. A colloidal suspension of solid particles in liquid is called "sol". A gel involves a successive solid skeleton enclosing a continuous liquid phase. The definition of a ceramic usually includes non-metallic and inorganic substances. Sol-gel method is able to supply flexibility in shaping sensor configuration during the polymerization process and simple method of immobilizing organic samples in porous matrices [11].

Sol-Gel Process

The sol-gel process includes the production of inorganic matrices through the formation of a colloidal suspension and then gelation of the sol to develop a wet gel. After wet gel dries, the gel state is called dry gel (xerogel). Drying by evaporation will lead to capillary pressure that causes shrinkage of the gel network. Usually the resulting dried gel is reduced volume by a factor of 5 to 10 times that is compared to the original wet gel. Most of sol-gel methods employ water and low molecular weight alkoxides such as tetramethoxysilane (TMOS, $Si(OCH_3)_4$), Tetraethoxysilane (TEOS,$Si(OC_2H_5)_4$), or an other organometallic alkoxide as a sol precursor. Generally alkoxides are polymerized in an alcohol/water solution with dissolved acids or bases to form a silica glass material [11]. The hydrolysis and condensation of a silicon alkoxide to form silica colloidal sol solution can be described by the following reactions.

hydrolysis,

$$Si(OR)_4 + nH_2O \leftrightarrow Si(OR)_{4-n}(OH)_n + nROH \quad (3.1)$$

alcohol condensation,

$$\equiv Si - OR + HO - Si \equiv \leftrightarrow Si - O - Si \equiv + ROH \quad (3.2)$$

water condensation

$$\equiv Si - OR + HO - Si \equiv \leftrightarrow Si - O - Si \equiv + H_2O \quad (3.3)$$

After condensation reaction, these monomers are able to form a complex branching network by the mechanism of polymerization.

Overall the net reaction can be expressed as:

$$nSi(OR)_4 + 2nH_2O \rightarrow nSiO_2 + 4nROH, \quad (3.4)$$

Gelation

The hydrolysis and polycondensation reactions happen at numerous sites within the TMOS and water mixture upon mixing. When sufficient interconnected Si-O-Si bonds are formed in region they respond cooperatively as colloidal particles, e.g. a sol. This sol is a relatively low viscosity liquid. With time, the colloidal particles sand condensed silica species link together to together to become a three dimensional network. The gel point is the time (reaction or degree) when the last bond is made that achieves this giant complex branching network [11, 10]

Drying and Aging

The expression aging is defined as the procedure of change in structure and properties after gelation. During the last periods of gelation, inorganic solvent and water

vaporize from the silica glass matrices and typically the volume of the solid matrix shrinks to around 10% of its original volume [11].

Some of the advantages of using sol-gel technique are:

1) Inorganic matrix synthesized by sol-gel process usually has much better thermal and chemical stability than organic polymer system

2) The surface area and porosity of sol-gel materials can easily be controlled so a suitable pore size can be designed

3) The good optical transparency of most sol-gel materials enable their usage with optical requirements, such as optical sensor [10]

4) Can easily shape materials in a gel state

5) High degree of homogeneity

Optical Properties of Sol-Gel Silica

Sol gel silica is transparent to visible and near infrared light as shown in the Figure 3.1. In deep ultraviolet region (UV) range, sol gel silica is opaque due to light being scattered by Rayleigh scattering given by:

$$T=A\,e^{\frac{-C\cdot t}{\lambda^4}} \tag{3.5}$$

where, T is transmittance, A is wavelength independent factor, C is intensity of Rayleigh scattering, t is the sample thickness, and λ is the wavelength.

The pores inside the sol gel silica act as scattering centers. A scattering center can be as small as single large molecule with an inherent inhomogenity, or clusters of small

molecules arranged in a non-uniform way. In the visible and near infrared regions, geometric scattering is prominent because of sol-gel silica's amorphous structure. In this region, sol gel silica is an adequate optical material [13].

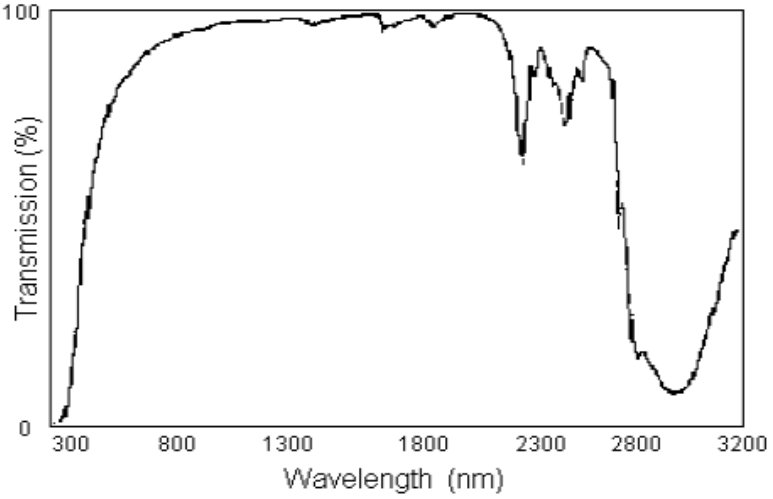

Figure 3.1: The light transmission of porous silica. The transmission in the graph is the fraction of light intensity transmitted through porous silica

Sol-Gel Derived Materials

Sol-gel derived materials can be prepared by dying the sol at different temperature. When the "sol" is cast into a mold, a wet "gel" will form. With further drying and heat-treatment, the "gel" is converted into dense ceramic or glass articles. When the wet-gel is dried at low temperature (25-100 C), a porous solid material called xerogel is obtained. Supercritical drying gives aerogels, which are highly porous and have low density. Thin films and coatings can be produced on a piece of substrate by spin-coating or dip-coating. As the viscosity of a "sol" is adjusted into a proper viscosity range, ceramic fibers can be drawn from the "sol". Ultra-fine and uniform ceramic

powders are formed by precipitation, spray pyrolysis, or emulsion techniques. Fiber optics can be used in conjunction with the monolith sol-gel sensing to provide feasible platform for chemical analysis [12, 11].

Sol-Gel Derived Hybrid Materials

Hybrid materials formed by the combination of inorganic materials and organic polymers are attractive for the purpose of creating high-performance or high-functional polymeric materials. Sol-gel technology, which is mainly based on inorganic polymerization reactions, is an important way to synthesize organic/inorganic hybrid materials. This is mainly because of its unique low temperature processing characteristic, providing opportunities to let organic and inorganic phases mix well and incorporate with each other at temperatures under which the organic phase can survive. Unlike conventional composites with inorganic or organic phase domains at millimeter or micrometer scale, the most of hybrid materials by sol-gel process are nanoscopic, with phase domain size in nanometer scale. Therefore, they are often optically transparent. Furthermore, via sol-gel process various kinds of bonds between organic and inorganic phases can be introduced, enhancing the interactions between two the phases.

Dependent on structural differences, organic/inorganic hybrid materials can be grossly divided into two classes:

Class I: The organic phase is physically embedded inside the inorganic matrix. The synthesis of this class of materials is usually carried by formation of inorganic network

backbone in presence of preformed organic phase, like prepolymer. Thus, only weak bonds can be formed between these two phases.

Class II: The organic and inorganic phases are covalent bonded. In this approach, the inorganic precursors must carry functional groups, which can react with organic phase during or after sol-gel process [10].

Applications

Sol-gel processing is particularly attractive for its ability to process such nanocomposite structures in the form of thin films for optoelectronic applications. Porous materials further allow for the fixation of organometallic complexes for heterogeneous catalysis, providing for easy recovery of catalysts and shape- and size-selectivity associated with the pore structures [14].

Sol-gel based sensors find numerous applications in chemical and biological areas. Due to wide flexibility in tuning chemical properties of sol-gel films along with superior mechanical and chemical stability, organically modified sol-gels represent highly interesting coating materials for mid-infrared sensing applications [20]. The sol-gel process is used for coating an unclad portion of an optical fiber with a microporous glass film where analyte-sensitive dyes are entrapped and into which smaller analyte molecules may diffuse. The benefits of this sol-gel approach to sensor fabrication are illustrated by results from a range of sensors for pH, ammonia and oxygen based on both evanescent wave absorption and evanescent wave excitation of fluorescence [21]. Porous silicate materials made by low temperature sol-gel process are promising host matrices

for encapsulation of biomolecules like enzymes, antibodies and cells. Their mechanical strength, chemical inertness, hydrophilic nature, and above all, their optical transparency makes them an exciting platform for development of biosensors [15].

CHAPTER IV

SEMICONDUCTOR QUANTUM DOT

Quantum dots are crystals composed of periodic groups of II-VI, III-V, or IV-VI elements [7]. They have dimensions of only 1 to 100 nanometres and contain somewhere between 10^3 and 10^6 atomic nuclei in a crystalline lattice [8]. An electron in a quantum dot can be described by a quantum wavefunction which is similar to that used for an electron in a single atom, even though its energy is spread coherently over the lattice of atomic nuclei. The importance of semiconductors, large or small, lies primarily in the great change in their properties when the number of active electrons in the material is altered. The electron density can be controlled with high sensitivity through doping, optical excitation or external electric fields [8]. The electrons in bulk (much bigger than 10 nm) semiconductor material have a range of energies. In bulk, energy levels are very close together, so close that they are described as continuous, meaning there is almost no energy difference between them. When the sizes of these dots become comparable to or smaller than the bulk exciton Bohr radius, then, the electron energy levels can no longer be treated as continuous. They must be treated as discrete, meaning that there is a small and finite separation between energy levels. This situation of discrete energy levels is called quantum confinement. Under these conditions, the semiconductor material ceases to resemble bulk, and instead can be called a quantum dot. Here the size of the bandgap is

controlled simply by adjusting the size of the dot which gives rise to unique optical and electronic properties.

Adding shells to these quantum dots surrounds the core completely and results in a significant increase in the quantum yield. It reduces nonradiative recombination and results in brighter emission, provided the shell is of a different semiconductor material with a wider bandgap than the core semiconductor material [7].

The absorption and photoluminescence spectra of CdSe and core-shell CdSe/ZnS nanocrystals are shown in Figure 4.1. The first absorption maximum of CdSe nanocrystal is observed at 571 nm. The mean particle diameter is 4.2 nm according TEM (Transmission Electron Microscope) as shown in Figure 4.2 (a) [6]

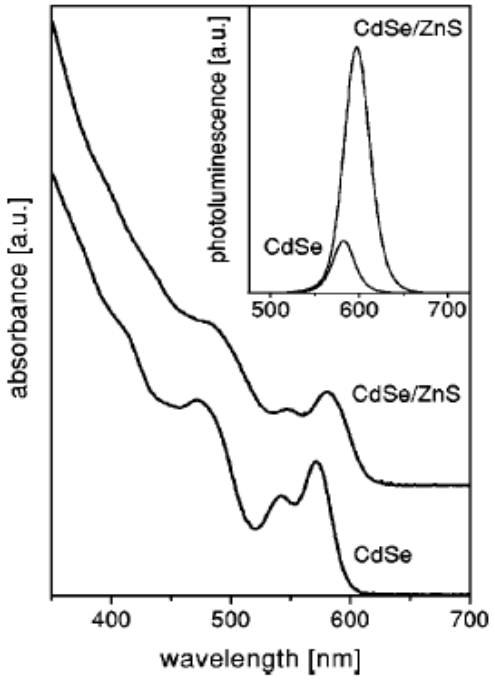

Figure 4.1 Absorption and photoluminescence spectra of the CdSe and Cdse/ZnS core-shell nanocrystals

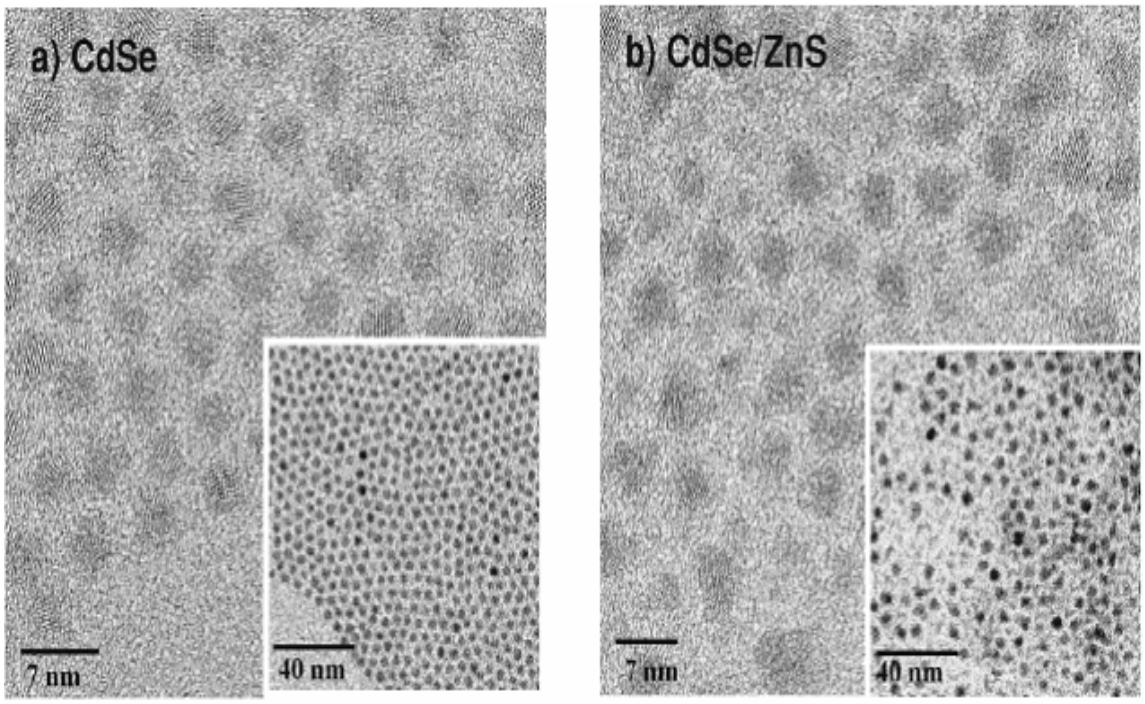

Figure 4.2: Overview and high resolution transmission electron microscope of a) CdSe and b) CdSe/ZnS core-shell nanocrystals

Advantages of Using Quantum Dot

1) The nanocrystal materials are very stable and have fine spectral resolution due to their narrow full width half maximum (FWHM)
2) Have broader absorption profile compared to traditional organic dyes and phosphors
3) The peak excitation wavelength does not overlap with emission wavelength
4) Fluoresce intensely and exhibit high quantum yields
5) CdSe/ZnS nanocrystals have 15-20 ns fluorescence lifetimes
6) Have a very flexible surface chemistry that can be altered for various applications to allow solubility in organic and aqueous solutions [7]

Applications

Quantum dots find a number of applications as electroluminescent devices for nano and bio sensors. Quantum dots attached to DNA probes provide a rapid and highly sensitive method for detecting small amounts of specific DNA sequences. These are used to capture specific DNA targets, concentrate them, and provide a strong fluorescent signal [22]. in optical detectors, quantum LED's, white light sources and quantum lasers, solar cells. Quantum dot nano-particles are used as temperature probes in luminescence chemical sensing applications. Results show the feasibility of implementing a self-referenced intensity-based sensor to perform temperature measurements independent of the optical power level in the sensing system [23]. Quantum dots find applications in imaging of lymphatic, vascular and tumor cells in multi-cellular animals. To apply quantum dots to biological detection and imaging applications, quantum dots are conjugated to molecules (e.g. peptide ligands, carbohydrate, antibodies, small molecule ligands) that can specifically recognize the biological target under study [24].

CHAPTER V

PREPARATION OF SCINTILLATING FIBERS

Preparation of Liquid Core Waveguide Fiber

A liquid core waveguide is a special optical fiber in which a liquid filled in a special capillary acts as a light guiding medium. A liquid core scintillating optical fiber was prepared using a special capillary TSU 100375; purchased from Polymicro Technologies (Phoenix, AZ). The capillary has a UV transparent coating and is made of synthetic fused silica. The capillary was filled with the scintillating material, nanostructured quantum dot solution. These quantum dot consist of core-shell CdSe/ZnS materials purchased from Evident Technologies (Troy, NY).The quantum dots are suspended in a solvent of toluene. Two different quantum dots with wavelengths of 520 and 580 nm were used to to prepare the liquid core scintillating optical fibers. A CdSe/ZnS quantum dot solution was carefully filled into a 0.2m TSU 100375 capillary. The presence of gas bubble in the filled capillary must be avoided.

Liquid Core Waveguide Detector Probe

A conventional optical fiber (FT 300 UMT, Thorlabs, NJ) of appropriate length was inserted in a silica capillary. The capillary has an external diameter of 696 μm and internal diameter 532 μm and length of about 5cm. One end of the liquid core fiber with

the quantum dot solution was connected to one end of the conventional optical fiber inside the capillary. Both ends of the silica capillary and liquid core hollow fiber were glued to prevent the quantum dot from flowing out .The structure of the liquid core scintillating fiber is as shown in the Figure 5.1.

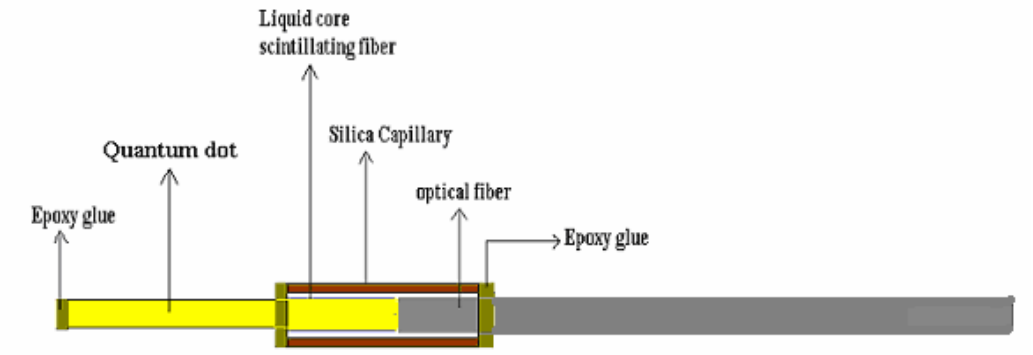

Figure 5.1: Liquid core scintillating fiber detector probe

Preparation of CsI and NaI Doped Silica Scintillating Fibers

Scintillating fibers were prepared from cesium iodide, sodium iodide pure and doped with NaI crystals (about 0.1%) in a sol-gel matrix. Preparation of a CsI or NaI doped silica scintillating optical fiber involved the hydrolysis of about 2ml of tetramethyl orthosilicate (TMOS) with 1ml of water for about an hour. Once the TMOS was hydrolyzed, a mixture of 300 mg of CsI (or NaI) and 1.5 ml water was added to the obtained silica sol solution as a dopant. This doped silica sol solution was filled in a tygon tube. The solution inside the tube gelled to form a gel fiber. The gel fiber was then pushed out of the tube by injecting water with a syringe. The gel fiber was then air-dried.

CsI/NaI Doped Silica Fiber Probe Detector

Sodium and cesium iodide doped silica scintillating fibers prepared by the process mentioned above were fabricated in the form of a detector probe. A scintillating fiber of diameter approximately 650 µm was placed in a silica capillary of internal and external diameter 693 and 850 µm respectively. A conventional silica optical fiber (FT 300 UMT, Thorlabs, NJ) was connected to one end of the scintillating fiber inside the capillary. Both ends of the capillary were then glued to form CsI/NaI doped silica scintillating fiber detector probe shown in the Figure 5.2.

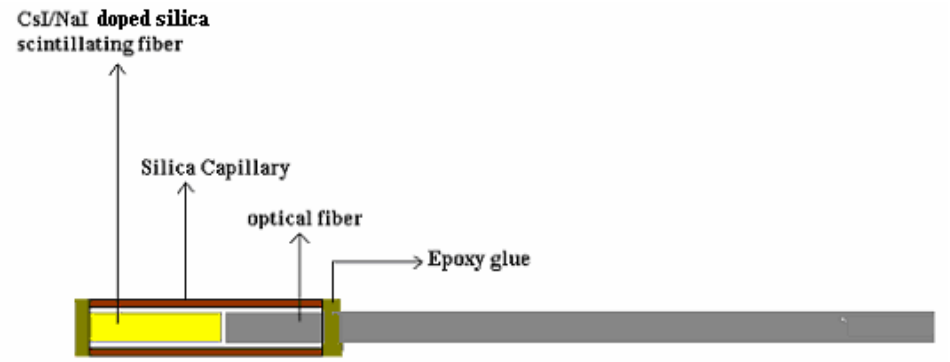

Figure 5.2: CsI/NaI doped silica scintillating fiber detector probe

Connecting a Scintillating Optical Fiber Sensor Probe to a PMT

The photomultiplier tube used is HC 137-11 (Hamamatsu Photonics, NJ), which has a head on photon counting module using R1924A select. A computer program (EvalVB10 software) was used to acquire the photon counts. The PMT has an integrated microcontroller, which provides excellent sensitivity, flexibility and accuracy. This PMT is directly connected to a personal computer via a serial port (RS-232) for communication

as shown in Figure 5.3. When the scintillating photons hit the cathode of the PMT, they are converted to current pulses. These pulses are amplified and converted to digital pulses with a high speed amplifier and discriminator that are built-in the PMT module. The output digital counts are acquired for recording and analysis using the software EvalVB10.

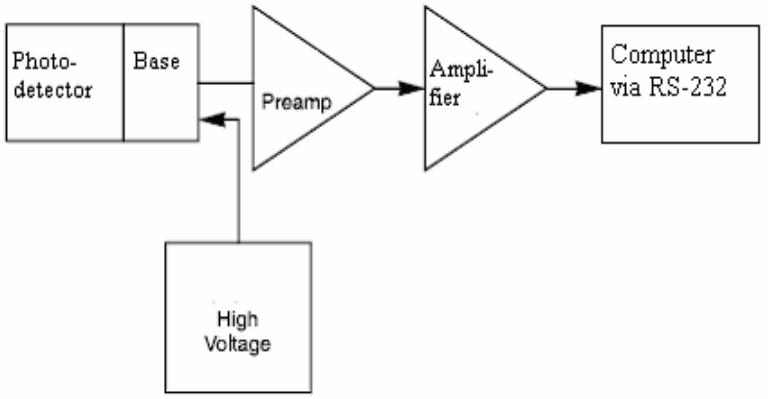

Figure 5.3: A circuit diagram of PMT module connected to a computer

CHAPTER VI

EXPERIMENTAL SET-UP

In order to test a scintillating fiber probe, the scintillating fiber was placed inside a gamma source (^{137}Cs) chamber. The free end of the conventional optical fiber probe was connected to the PMT, which is located outside the gamma source chamber as shown in Figure 6.1. The scintillating fiber probe was deployed into a black tube and was coupled to the photomultiplier tube. This black tubing is required to prevent external light from entering the fiber and causing an increase in background count. This tubing runs throughout the length of the scintillating probe detector. The PMT was also completely shielded with a black box to keep away stray light from entering inside and to minimize the background counts.

During the test the dose of gamma radiations was increased step by step and the PMT counting signal was recorded.

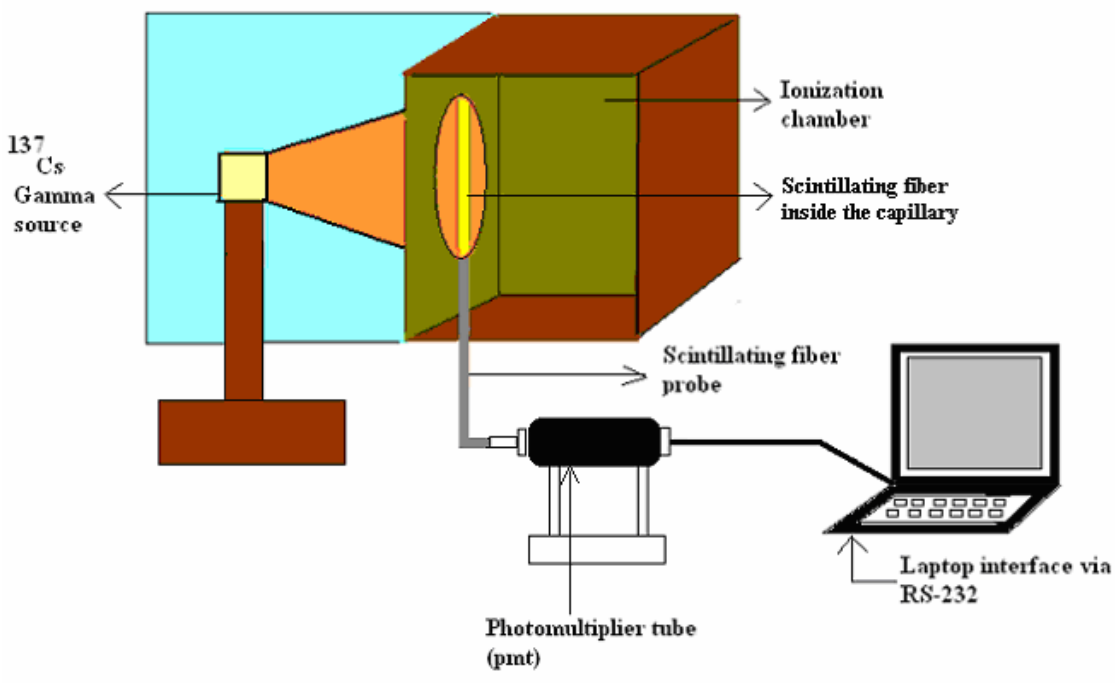

Figure 6.1: Schematic of the experimental set-up

CHAPTER VII

RESULTS AND DISCUSSION

When the light enters the photocathode of the PMT, photoelectrons are emitted from the photocathode. These photoelectrons are multiplied by the secondary electrons emission through the dynodes and then collected by the anodes as an output pulse. The output peak current I_p from the PMT can be calculated as:

$$I_p = e\,\mu\,\frac{1}{t}\,A \tag{7.1}$$

where e=electron charge ($1.6*10^{-19}$C), μ is the gain of the PMT, t is the pulse width (FHWM), A is unit of current in Amperes

These short current pulses are amplified and converted to digital pulses with a high speed amplifier and discriminator. These counts correspond to the incident gamma radiation. The radiation counts produced in the scintillating fiber probes with NaI, CsI, CsI(Na), quantum dot and the commercial scintillating fiber is shown in Table 7.1. The unit of radiation exposure of gamma source is given by Roentgen per hour(R/hr), which is the quantity of gamma radiation that will produce one electrostatic unit of electricity in one cubic centimeter of dry air at standard temperature and atmospheric pressure. The number of sampling time represents the time taken by the PMT circuit for one analog to digital conversion of the scintillator output response.

Table 7.1: Test Results of Scintillating Fibers as Recorded from HC135-11 PMT Module

Gamma source reading (R/hr)	Photon counts (cps) Peak value of NaI	Photon counts (cps) Peak value of CsI	Photon counts (cps) Peak value of CsI doped with Na	Photon counts (cps) Peak value of Quantum Dot	Photon counts (cps) Peak value of Commercial scintillating fiber
0	80	181	52	72	64
0.33	160	264	76	188	80
3.62	296	384	148	348	216
36.38	1600	1696	1024	1596	1588
376.49	16100	14764	9360	15364	15844

Initial experiments were carried out with liquid core waveguide fiber detector probe filled with saturated solution of anthracene and fluoranthene as a scintillating material. These probes were fabricated in a similar way as the liquid core waveguide detector probe using quantum dot solution. For the fluoranthene solution filled liquid core waveguide fiber, the result as seen in Figure 7.1, indicates that this flouranthene solution based scintillating optical fiber does not respond to gamma radiation. There is no obvious light signal being detected even when the probe was exposed to 376.5R/hr. Therefore this indicated that fluoranthene is not a suitable material for preparing liquid core scintillating fiber detector probe.

Anthracence, which is one of the well known liquid scintillating material, was filled in a liquid core fiber waveguide and prepared as a scintillating fiber probe. The

results shown in Figure 7.2 indicate that the maximum photon counts corresponding to the incident radiation energy is around 800 counts, for the radiation dose input of 376.5R/hr from the gamma source.

Figure 7.3 shows the test results from the quantum dot liquid core scintillating detector probe. The quantum dot solution used has a wavelength of 520nm. As seen in the results, the maximum counts observed were nearly 6700 at 376.57R/Hr. This proves that the quantum dot solution was a much better choice in the preparation of the liquid core scintillating fiber detector probe.

A commercial scintillating fiber was tested in the same method as the other scintillating fiber probes to compare the sensitivity of the scintillating fibers prepared in this work with the commercial plastic scintillating fiber. The commercial scintillating fiber used is BCF20 purchased from Bicron, OH. It is a plastic scintillating fiber with peak emission~492nm. The test result from this plastic scintillating fiber is shown in Figure 7.4.

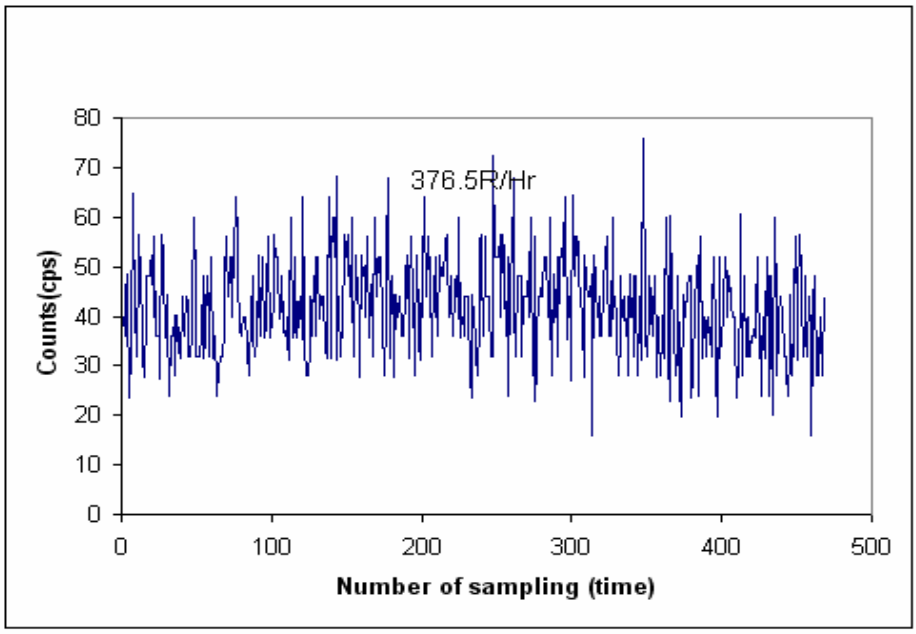

Figure 7.1: Radiation counts (Roentgen/Hr) of Fluoranthene liquid core scintillating fiber

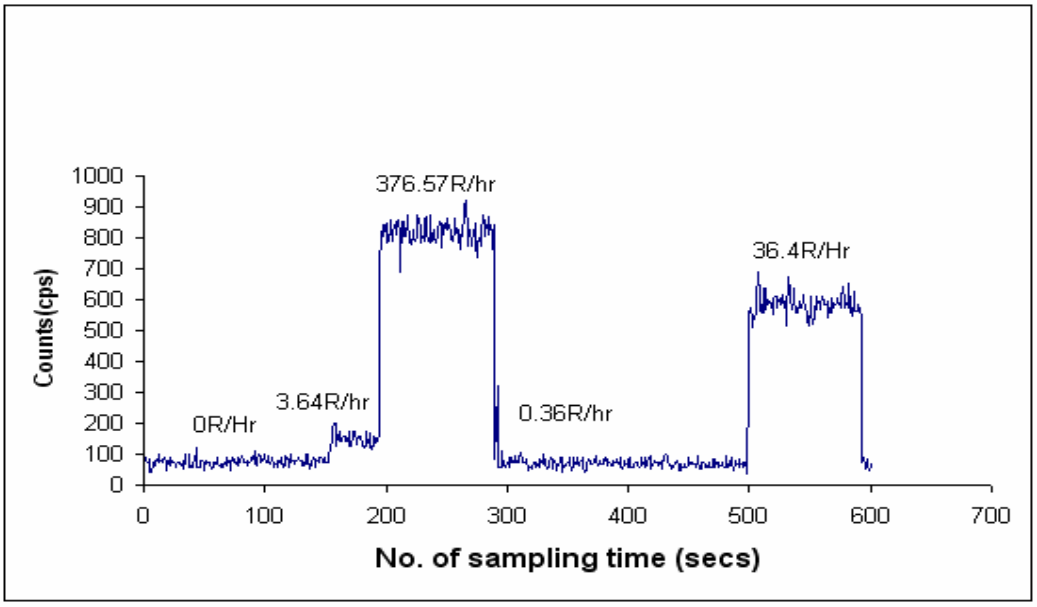

Figure 7.2: Radiation counts (Roentgen/Hr) of Anthracene liquid core scintillating fiber

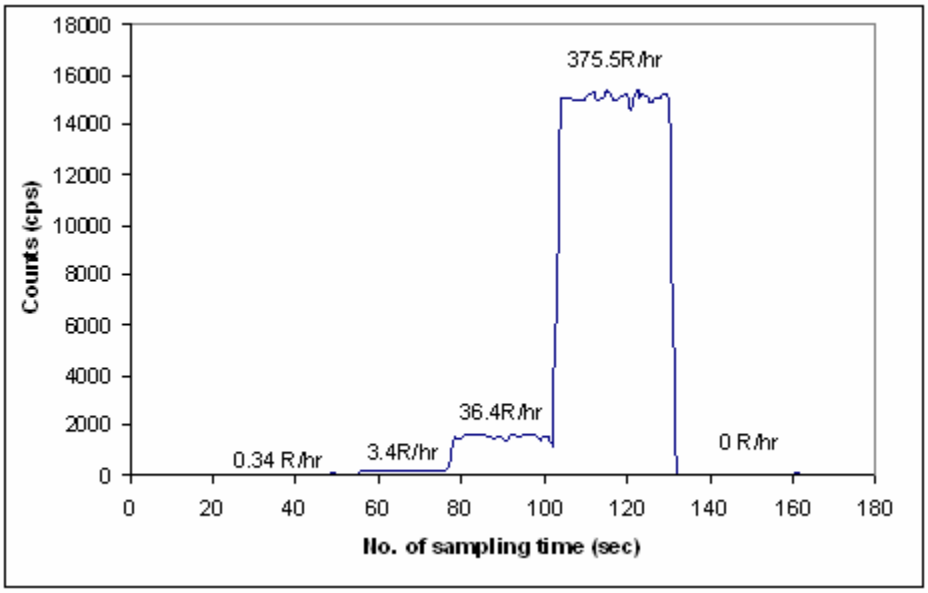

Figure 7.3: Radiation counts (Roentgen/Hr) of Quantum Dot liquid core scintillating fiber

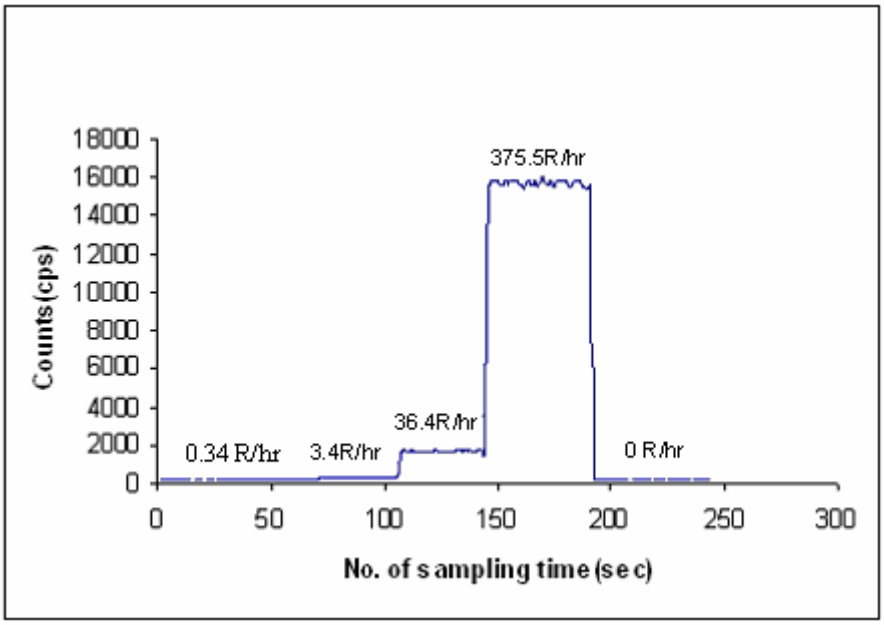

Figure 7.4: Radiation counts (Roentgen/Hr) of Commercial scintillating fiber

The test results of silica scintillating optical fibers doped with NaI, CsI, Cs(Na) are shown in Figures 7.5 through 7.7. These inorganic scintillating agent doped scintillating optical fibers are sensitive for gamma ray detection. The sensitivity of these fibers is comparable with that of the commercial plastic scintillating fiber. However, it should be mentioned that the composition of these silica scintillating optical fibers has not been optimized. It was observed that the sensitivity of these scintillating optical fibers depends on the concentration of the inorganic scintillating agent.

For example, in the case of CsI and NaI doped silica scintillating fiber it was observed that the scintillating light output varied with different concentrations of the scintillating material (NaI, CsI and CsI(Na)). The fibers doped with about 0.6% of both CsI and NaI (0.3g each) showed better light output and efficiency than 1% of both CsI and NaI (0.5g each) shown in Figure 7.8. It is expected that silica scintillating optical fiber having more NaI or CsI doping should have higher sensitivity for gamma ray detection. The observed results can be explained as a side chemical reaction. Fibers with more concentration of iodine in NaI or CsI tend to become brown with prolonged drying in the presence of air due to the oxidation of iodide ions to iodine given by the equation:

$$4I^- + O_2 + 4H^- \leftrightarrow 2I_2 + 2H_2O \quad \text{.....} \quad (7.2)$$

The presence of the brown colored iodine makes the scintillating fibers partially opaque, which in turn, decreased the light output. Therefore the sensitivity of these silica scintillating optical fibers can be improved through optimizing fiber fabricating process. The sensitivity of the NaI, CsI, CsI(Na) doped silica scintillating fibers and quantum dot

scintillating fiber could still be improved by increasing the diameter of the fibers and optimizing the procedure of fiber fabrication process.

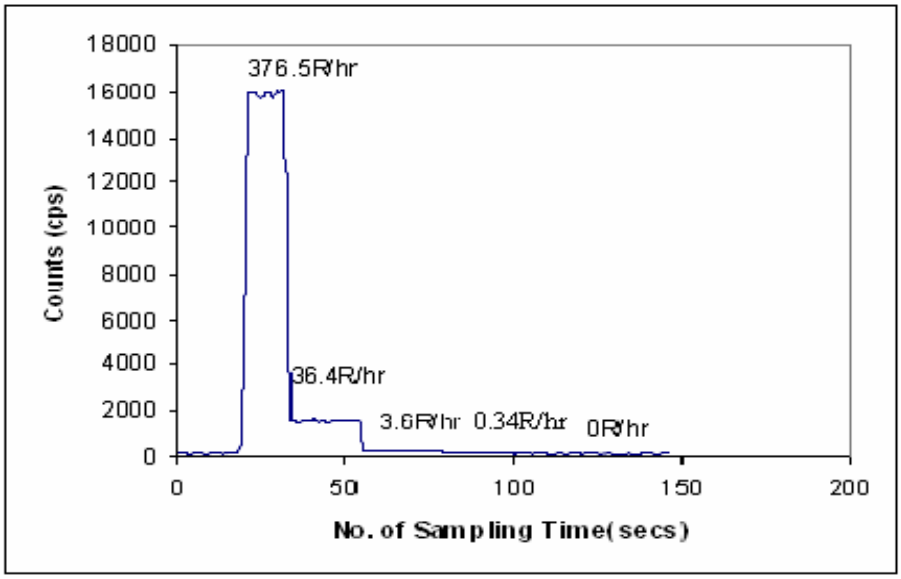

Figure 7.5: Radiation counts (Roentgen/Hr) of NaI doped silica scintillating fiber

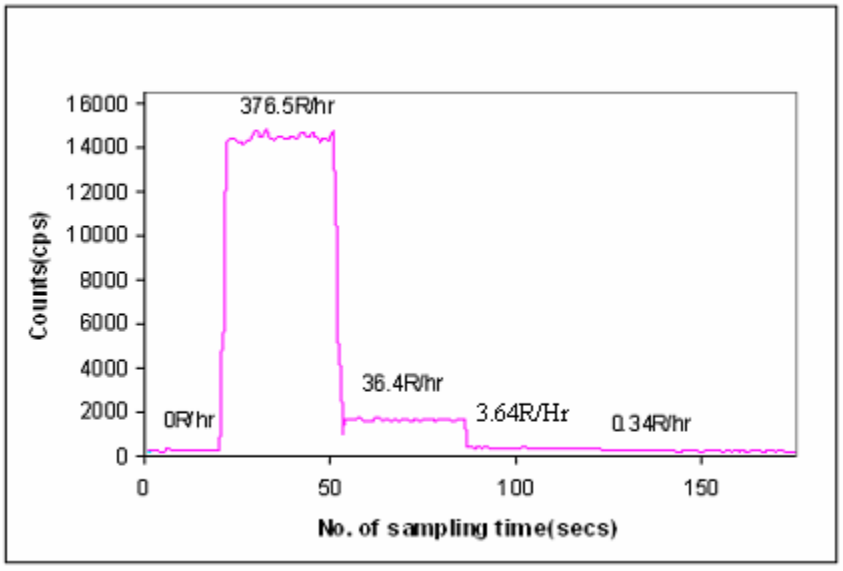

Figure 7.6: Radiation counts (Roentgen/Hr) of CsI doped silica scintillating fiber

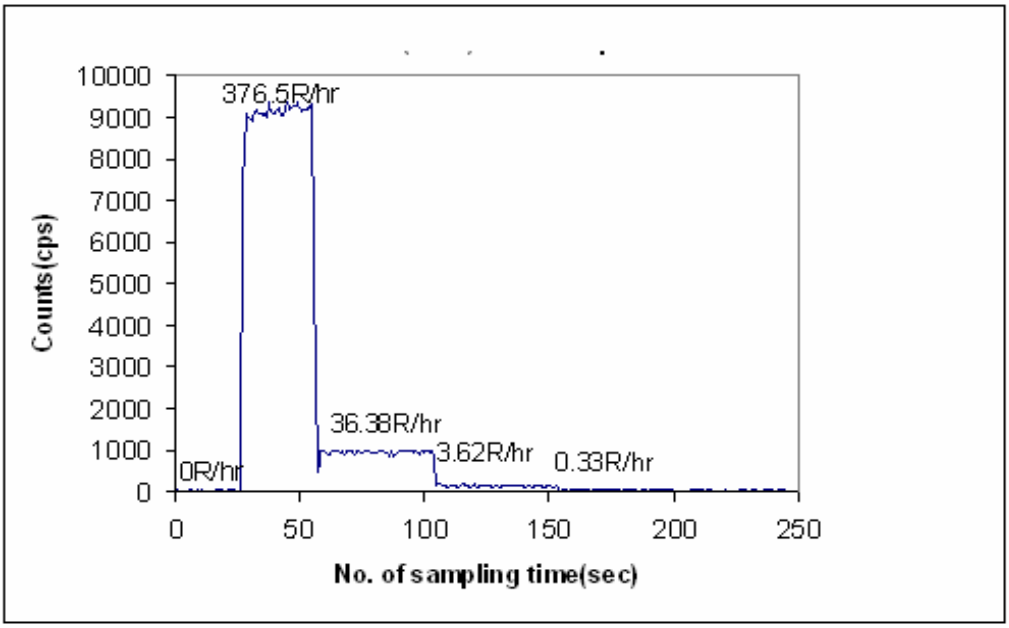

Figure 7.7: Radiation counts (Roentgen/Hr) of CsI(Na) doped silica scintillating fiber

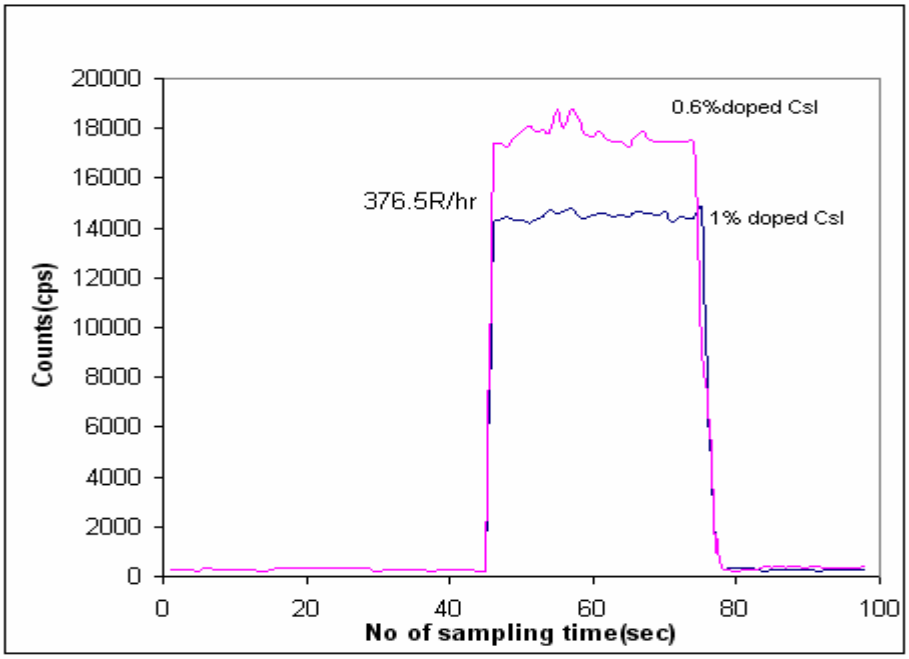

Figure 7.8: Radiation counts (Roentgen/Hr) of CsI doped silica scintillating fiber with different concentrations

Calibration

The calibration curves shown in Figures 7.9 through 7.13 for the scintillating fiber sensors of this work were obtained by using a regression fit. The results shown in figure show a linear relationship between the radiation dose exposure in Roentgen per hour and the photon counts per sec output from the PMT, for all the tested scintillating optical fiber detector probes. The detection limits (D.L) of the scintillating fibers have been calculated using the equation:

$$D.L = \frac{3\sigma}{\text{slope of the calibration curve}} \tag{7.3}$$

where σ is the standard deviation of the PMT output without gamma radiation

Table 7.2: Detection Limits Obtained for the Tested Scintillating Fibers of this Work

Scintillating Fiber	Detection Limit (D.L)
CsI	2.242428
CsI/Na	1.821646
NaI	2.371688
Quantum Dot	4.608341

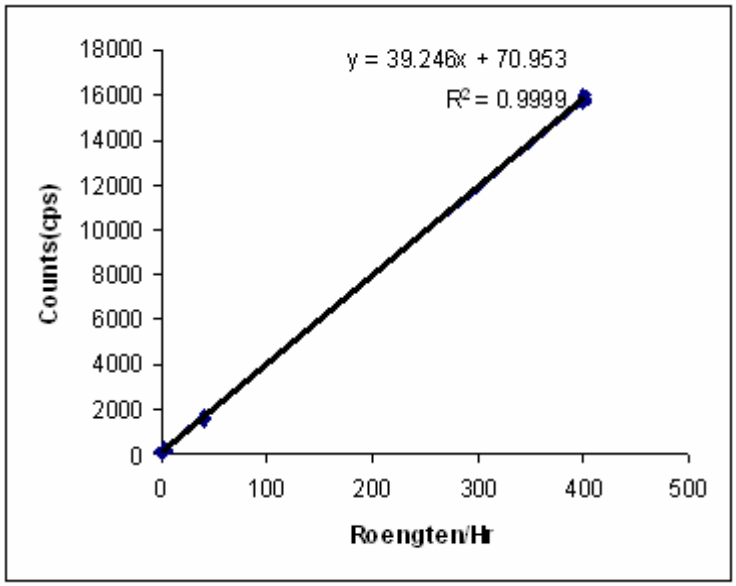

Figure 7.9: A calibration curve of Commercial scintillating fiber for detecting gamma radiation quantitatively

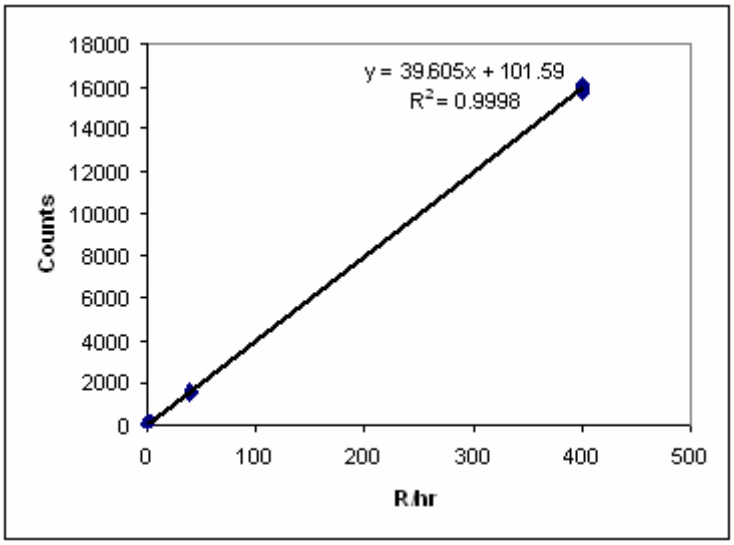

Figure 7.10: A calibration curve of NaI doped silica scintillating fiber for detecting gamma radiation quantitatively

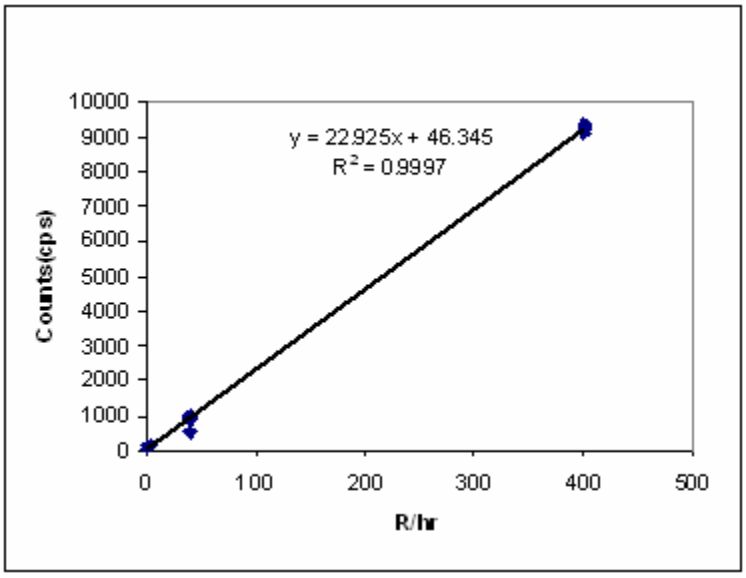

Figure 7.11: A calibration curve of CsI(Na) doped silica scintillating fiber for detecting gamma radiation quantitatively

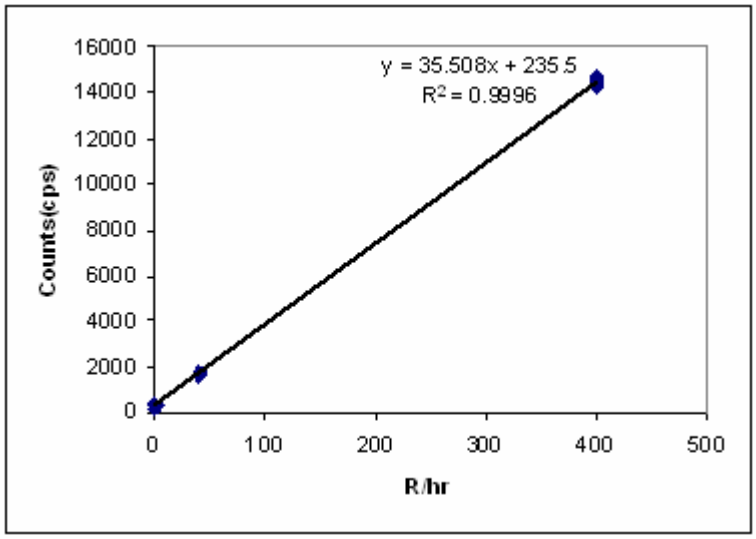

Figure 7.12: A calibration curve of CsI doped silica scintillating fiber for detecting gamma radiation quantitatively

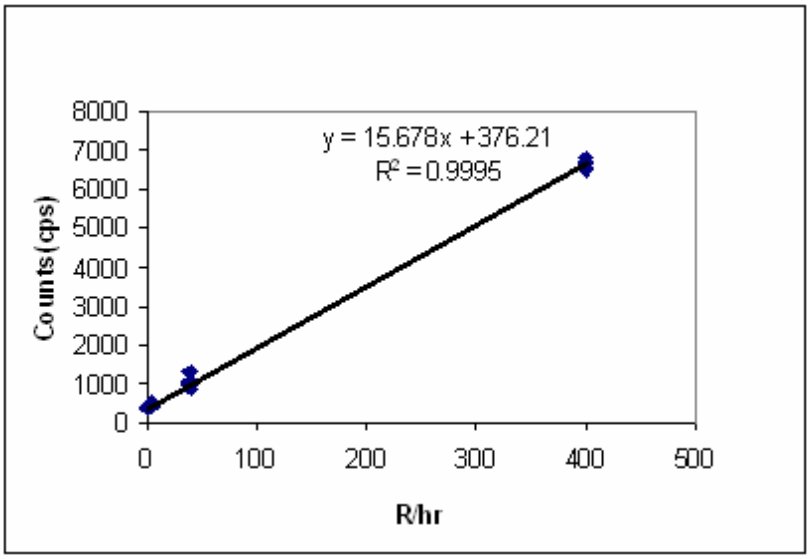

Figure 7.13: A calibration curve of Quantum Dot solution filled scintillating fiber for detecting gamma radiation quantitatively

CHAPTER VIII

POTENTIAL APPLICATIONS OF THE SCINTILLATING FIBER DETECTOR

Scintillating fiber probes can find many potential applications due to their low cost and ease of preparation, high density and efficiency, size and compactness compared to other scintillation counters.

These detectors could be used for a variety of applications which include gamma-ray spectroscopy, contamination surveys, land surveys and aerial radiological surveys for the presence of gamma- emitting radionuclides.

They can be used for safety detector requirements like in a scanner to rapidly identify a suspect luggage in a few cubic meter large container moving across the inspection device and remote detection of fissile materials [19]. These detectors can be used for DoD's requirements for laboratory applications, such as nuclear material processing, laboratory research activity, to field applications such as nuclear waste processing and management, nuclear explosion monitoring, maritime security and radioactive material transportation monitoring.

Scintillating fibers could find applications in medical imaging techniques, where a radioisotope is injected into the body, which produces ionizing radiation that can be detected by inserting a scintillating fiber sensor into the diseased part. Scintillating fibers can also be used in the form of an array for imaging purposes in order to determine

something about the physiology or anatomy of the target organ. Thus, it is possible to determine whether the biochemical function of an organ is impaired when compared to other forms of medical imaging like x-ray, ultrasound or magnetic resonance techniques where only the physical structure of an organ can be determined. Finally scintillating fiber probes can be placed in a surgical opening left after all the cancerous cells are removed, to determine if the surrounding cells around the tumor has high radiotracer concentration [17].

REFERENCES

[1] Herman Cember, "Introduction to Health Physics," Pergamon Press, 105, 1969, pp.181-185.

[2] Hugh F Henry, "Fundamentals of Radiation protection," Wiley Interscience, 1969, pp.206

[3] Glenn F. Knoll, "Radiation Detection and Measurement," John Wiley & Sons, 1989

[4] R. Chipaux, M. Geleoc, P. Bellevil, "Sol-gel coating of scintillating crystals," IEEE Transactions Nuclear Science, 47, no.6, 2000

[5] J.B. Kirks, "Scintillation Counters," McGraw Hill Book Co., Inc, 1953

[6] H.Borchert and D.V.Talapin, C.McGinley, S.Adam, and A. lobo, A.R.B. de Castro, T.Moller, H.Weller, "High resolution photoemission study of CdSe core-shell nanocrystals," Journal of Chemical Physics, 119, no.3, 2003

[7] http://www.evidenttech.com/qdot-definition/quantum-dot-about.php

[8] Daniel Gammon, "Electrons in artificial states," Nature, 405, 2000, pp.899 – 900

[9] S.E. Letant and T.F.Wang, "Study of porous glass doped with quantum dots or laser dyes under alpha irradiation," Applied Physics Letters, 88, 2006

[10] Sun, Zhengfei, "Novel sol-gel nanoporous materials, nanocomposites and their applications in bioscience", Drexel Theses and Dissertations, 2005, pp.42-43

[11] Po-Chun Chang, "Sol-gel based fluorescence sensor for calcium", UMI Microform, 1389391, 1998, pp.32-35

[12] http://www.chemat.com/html/solgel.html

[13] Lina Xu, "Optical fiber humidity sensor based on evanescent wave scattering," Thesis and Dissertation, Mississippi State University, 2004, pp.16-17

[14] Jackie Y. Ying, “Chemistry of materials,” The American Chemical Society, 9, no.11, 1997

[15] Anup K Singh, Alok Gupta, Ashok Mulchandani, Wilfred Chen, Rimple B Bhatia,Joseph S Shoeniger, Carol S Ashley,C.J. Brinker, “Encapsulation of enzymes and cells in sol-gel matrices for biosensor applications,” Proceedings SPIE , Advanced Materials and Optical Systems for Chemical and Biological Detection, 3858,1998, pp. 10

[16] Shinzou Kubota, Hiroyuki Murakami, Jian-Zhi RUAN (Gen) and Naohito IWASA, Shiro Skuragi, Santoshi Hashimtoto, “The new scintillation material CsI and its application to position sensitive detectors”, Nuclear Instruments and methods, A273, 1988,pp. 645

[17] William W.Moses, “Overview of Nuclear Medical Imaging Instrumentation and Techniques,”SCIFI97: Conference on Scintillating Fiber Detectors, 1997, pp.477, 485

[18] Piotr A.Rodnyi, “Physical Processes Inorganic Scintillators,” CRC Press, 1997

[19] Paul lecoq, Alexander Annenkov, Alexander Gektin, Mikhail Korzhik, Christian Pedrini, “Inorganic Scintillators for Detector Systems,” Physical Principles and Crystal Engineering, Springer 20006

[20] Janotta Markus, Katzir Abraham, Mizaikoff Boris, “Sol-gel-coated mid-infrared fiber-optic sensors,” Applied spectroscopy, 57, no. 7, 2003, pp. 823.

[21] B. D. Mac Craith, C. Mcdonagh, G. O" Keeffe, T. Butler, B. O" Kelly and J. F. Mcgilp, “Fibre optic chemical sensors based on evanescent wave interactions in sol-gel-derived porous coatings,” Journal of Sol-Gel Science and Technology, 2, no. 1-3, 1994, pp.661

[22] Chun-Yang Zhang, Hsin-Chih Yeh, Marcos T. Kuroki and Tza-Huei Wang**,** **“**Single-quantum-dot-based DNA nanosensor,” Nature Materials, 4, 2005, pp.826, 2005

[23] P. A. S Jorge, M. Mayeh, R. Benrashid, P. Caldas, J. L .Santos and F. Farahi, “Quantum dots as self-referenced optical fiber temperature probes for luminescent chemical sensors,” Measurement Science and Technology,17, 2006,pp. 1032

[24] Yan Zhang, Min-kyung So, Andreas M. Loening, Hequan Yao, Sanjiv S. Gambhir, and Jianghong Rao, “HaloTag Protein-Mediated Site-Specific Conjugation of Bioluminescent Proteins to Quantum Dots,” Angewandte Chemie International Edition**,** 45, 2006, pp 4936